PROCEEDINGS OF THE ROYAL SOCIETY A

Proc. R. Soc. A (2006) **462**, 3151–3166
doi:10.1098/rspa.2006.1719
Published online 16 May 2006

Writing and coiling of closed filaments

By Francesca Maggioni[1] and Renzo L. Ricca[1,2,*]

[1]*Department of Mathematics and Applications, University of Milano-Bicocca, Via Cozzi 53, 20125 Milano, Italy*
[2]*Department of Mathematics, University College London, Gower Street, London WC1E 6BT, UK*

The kinematics of writhing and coiling of circular filaments is here analysed by new equations that govern the evolution of curves generated by epicycloids and hypocycloids. We show how efficiency of coil formation and compaction depend on writhing rates, relative bending, torsion and mean twist energy. We demonstrate that for coiling formation hypocycloid evolution achieves higher writhing rates, but in terms of deformation energy, the epicycloid evolution is much more effective. We also show how the occurrence and multiple appearance of inflexional configurations determine coil formation. Compaction and packing rate are also briefly examined. These results are fundamental and provide useful information for physical applications and for modelling natural phenomena, including relaxation of magnetic fields in the solar corona, magnetic dynamos in astrophysical flows, tertiary folding of macromolecules in chemical-physics, and DNA packing in cell biology.

Keywords: kinematics of curves; coiling; writhing; twist; inflexional geometry; deformation energy

1. Introduction

In this paper, we present a careful analysis of the kinematics of writhing and coiling of circular filaments by examining different models of curve evolution. Starting from a set of governing equations that describe the time evolution of curves generated by epicycloids and hypocycloids, we show how the efficiency of coil formation (given by the kinematic effectiveness of producing coiling) and compaction mechanisms depend on writhing rates, relative bending, torsion and mean twist energy. This is done by performing a comparative analysis of the models considered and the numerical results. We demonstrate that for coiling formation hypocycloid evolution achieves higher writhing rates, but in terms of deformation energy the epicycloid evolution is much more effective. We also show how the occurrence and multiple appearance of inflexional configurations determine coil formation. These results are fundamental and provide important information to understand the role of geometric properties in several dynamical systems in nature.

Filamentary structures such as magnetic flux-tubes in magneto-hydrodynamics, vortex filaments in turbulent flows and DNA molecules in biology are just a few

* Author for correspondence (renzo.ricca@unimib.it).

Received 23 January 2006
Accepted 20 March 2006

examples of physical systems that exhibit, at very different scales, morphological changes that involve recurrent writhing and coiling. In astrophysical flows, magnetic dynamos can be produced by mechanisms that mimic localized writhing and folding of magnetic fields (see, for example, Moffatt & Proctor 1985; see also Childress & Gilbert 1995), while tertiary folding of macromolecules (Zhang *et al.* 1994; Baker 2000) and DNA packing in the cell (Calladine & Drew 1992; Stasiak 1996) pose questions of fundamental research in chemical physics and biology. These issues involve localized geometric re-arrangement of a filament, that is associated with re-distribution of internal energy (kinetic, magnetic or elastic) and minimization of localized surplus, by accommodating the energy in excess in a new configuration. In many instances, the evolution is driven by an energy minimization process that also involves conservation of topology, with conservation of topological quantities like knot type and linking numbers. In the case of a closed filament in isolation, for instance, conservation of the linking number Lk implies the invariance of the sum of two geometric quantities, the writhing number Wr and the total twist Tw, according to the well-known formula (Călugăreanu 1961; White 1969)

$$Lk = Wr + Tw. \tag{1.1}$$

The writhing number Wr is related to the coiling of the filament axis and the total twist Tw to the winding of the infinitesimal constituent fibres around the filament axis (for a precise definition of these two quantities see below). When topology is frozen, then $Wr + Tw = \text{constant}$, allowing a continuous exchange of Wr and Tw during evolution, through a continuous change of curvature and torsion of the filament axis, and of intrinsic twist of the filament fibres. In general, above a certain critical twist value (that depends on the particular physical situation), we have conversion of torsional energy into bending energy, a mechanism that typically tends to serve a double purpose: to trigger instability or lower its threshold (particularly so when Tw is very near to the critical value), and to produce a configurational re-arrangement by writhing, folding and compaction of the filament in its ambient space. These aspects are important in nature, either at a microscopic level, as in the case of the human DNA, where a molecule a few centimetres long can be stored in a micron-sized scroll of protein, or in the macrocosm, where through these processes we have the relaxation of magnetic fields, leading to solar flares and spontaneous intensification processes that lead to magnetic dynamos.

In this paper, we want to investigate relations between efficiency of writhing and coiling (given by the effectiveness of the model to perform coiling through folding), deformation energy and its localization and re-distribution. We also want to address these questions in relation to the appearance of multiple coils and subsequent filament compaction. To do this, we consider a closed filament $\mathcal{F}$, given by a thin tube of length L and uniform circular cross-section of area $A = \pi a^2$, with $L \gg a$. $\mathcal{F}$ is thought to be made of a bundle of infinitesimal helical fibres, distributed inside the tube and wound around the tube axis $\mathcal{C}$ with twist. We also assume that the filament be inextensible, so that $L = \text{constant}$. $\mathcal{C}$ is given by a smooth (at least C^3), simple (i.e. non-self-intersecting), closed curve $\boldsymbol{X} = \boldsymbol{X}(\xi)$ in $\mathbb{R}^3$, where $\xi \in [0,2\pi]$ is a parameter on the curve. The geometry of the axis is prescribed by the curvature $c = c(\xi)$ and torsion $\tau = \tau(\xi)$ of $\boldsymbol{X}$ through the Frenet–Serret formulae.

We shall consider global geometric quantities, which are useful to quantify the total amount of coiling, folding and twist present. The total amount of *coiling* is naturally measured by the normalized total curvature K, given by

$$K \equiv \frac{1}{2\pi}\oint_{\mathcal{C}} c(\xi)\|\boldsymbol{X}'(\xi)\|\mathrm{d}\xi, \tag{1.2}$$

where prime denotes derivative with respect to ξ; a useful measure of *folding* is given by writhing number Wr (Fuller 1971), defined by

$$Wr \equiv \frac{1}{4\pi}\oint_{\mathcal{C}}\oint_{\mathcal{C}} \frac{\hat{\boldsymbol{t}}(\xi)\times\hat{\boldsymbol{t}}(\xi^*)\cdot[\boldsymbol{X}(\xi)-\boldsymbol{X}(\xi^*)]}{|\boldsymbol{X}(\xi)-\boldsymbol{X}(\xi^*)|^3}\|\boldsymbol{X}'(\xi)\|\,\|\boldsymbol{X}'(\xi^*)\|\mathrm{d}\xi\,\mathrm{d}\xi^*, \tag{1.3}$$

where $\boldsymbol{X}(\xi)$ and $\boldsymbol{X}(\xi^*)$ denote two points on the axis for any pair $\{\xi,\xi^*\}\in[0,2\pi]$, and $\hat{\boldsymbol{t}}(\xi)\equiv\boldsymbol{X}'(\xi)/\|\boldsymbol{X}'(\xi)\|$ is the unit tangent to $\mathcal{C}$ at ξ.

The *total twist* Tw measures the total winding of the infinitesimal fibres around $\mathcal{C}$ and is known once the twist rate is prescribed everywhere along $\mathcal{C}$; denoting by $\Omega=\Omega(\xi)$ the angular twist rate, we have

$$Tw \equiv \frac{1}{2\pi}\oint_{\mathcal{C}} \Omega(\xi)\|\boldsymbol{X}'(\xi)\|\mathrm{d}\xi, \tag{1.4}$$

which is related to the geometry of the filament axis through the decomposition (see, for example, Moffatt & Ricca 1992)

$$Tw = \frac{1}{2\pi}\oint_{\mathcal{C}} \tau(\xi)\|\boldsymbol{X}'(\xi)\|\mathrm{d}\xi + \frac{1}{2\pi}[\Theta]_{\mathcal{F}} = \mathcal{T}+\mathcal{N}, \tag{1.5}$$

where the first term in the r.h.s. of equation (1.5) is the normalized total torsion $\mathcal{T}$ and the second term is the normalized intrinsic twist $\mathcal{N}$ of the fibres *around* $\mathcal{C}$ ($\boldsymbol{\Theta}$ being the total number of turns of twist). If we take the fibres to be closed, then $\mathcal{N}$ is an integer. Note that $K=K(\mathcal{C})$, $Wr=Wr(\mathcal{C})$ and $\mathcal{T}=\mathcal{T}(\mathcal{C})$, in the sense that they depend only on the geometry of the filament axis, whereas the total twist Tw and the intrinsic twist $\mathcal{N}$ depend also on the distribution of the fibres inside the tube (in this sense the reduction of (1.4) to a line integral can be misleading). This is evident when the curve $\mathcal{C}$ is a plane circle: in this case there is no contribution from torsion (since for the circle $\tau=0$ everywhere), and the total twist Tw coincides with the intrinsic twist $\mathcal{N}$.

2. Kinematic models of writhing and coiling formation

Efficient mechanisms of writhing and coiling formation are examined by comparing different kinematic models based on the time evolution of space curves that evolve from a plane circle. For this, we introduce a family of time-dependent curves $\boldsymbol{X}=\boldsymbol{X}(\xi,t)$ given by the extension to three-dimensions of well-known planar curves (see, for example, Lockwood 1961; Arganbright 1993); we propose the following set of governing equations:

$$\boldsymbol{X}=\boldsymbol{X}(\xi,t): \quad \begin{cases} x = a\cos(m\xi) + bf_1(t)\cos(n\xi), \\ y = c\sin(m\xi) + df_2(t)\sin(n\xi), \\ z = f_3(t)\sin(\xi), \end{cases} \tag{2.1}$$

Table 1. Types of generatrix curve, with reference to the *xy*-projection of equations (2.1), for different values of parameters, for $m=1$ and $n=2+4r$, where $r\in\mathbb{N}$. (Note that for these curves we have an upper bound on the writhing number given by $|Wr|_{\max}=1$. For $n=2+2r$, where $r\in\mathbb{N}$ is odd, we have the same curves, with relative range of writhing number exchanged.)

generatrix curve	a	b	c	d	Wr-range
epicycloid	$+1$	±1	±1	$+1$	$[-1,0]$
hypocycloid	$+1$	∓1	±1	$+1$	$[-1,0]$
epicycloid	$+1$	∓1	±1	-1	$[0,1]$
hypocycloid	$+1$	±1	±1	-1	$[0,1]$

where a, b, c, d take the value $+1$ or -1, $n>m>0$, with n, m integers and $f_i(t)$ ($i=1,2,3$) are time-dependent functions. For simplicity, we consider the simplest linear dependence on time given by $f_i(t)=t$ (here time is merely a kinematic parameter, while an appropriate time-dependent prescription will be dictated by the particular physical process considered).

The values ±1 for a, b, c, d exhaust in fact all possible cases and any different choice of these numbers will generate similar curves (homothetic configurations that are equivalent up to a scale factor). For given values of the parameters a, b, c, d (see table 1), equations (2.1) describe the time evolution of closed curves that originate (at $t=0$) from a plane circle of length $L=2\pi$ (since $a^2=c^2=1$), and evolve to form singly or multiply coiled configurations. According to the values of the parameters, we refer to an epicycloid or a hypocycloid type of curve and/or evolution, in relation to the corresponding type of plane curve (seen as the 'generatrix' of the specific kinematics) in the *xy*-projection.

Since we do not want to have stretching, we ensure filament inextensibility by normalizing $\boldsymbol{X}=\boldsymbol{X}(\xi,t)$ by the length function

$$l(t)=\frac{1}{2\pi}\int_0^{2\pi}\left[\left(\frac{\partial x}{\partial\xi}\right)^2+\left(\frac{\partial y}{\partial\xi}\right)^2+\left(\frac{\partial z}{\partial\xi}\right)^2\right]^{1/2}\mathrm{d}\xi. \tag{2.2}$$

Note that, equation (2.2) cannot be integrated in closed form, so that $\boldsymbol{X}=\boldsymbol{X}(\xi,t)$ cannot be parametrized by arc-length. Hence, we shall replace the former set of equations (2.1) with the following:

$$\boldsymbol{X}=\boldsymbol{X}(\xi,t):\quad\begin{cases}x=[a\cos(m\xi)+bt\cos(n\xi)]/l(t),\\ y=[c\sin(m\xi)+dt\sin(n\xi)]/l(t),\\ z=[t\sin(\xi)]/l(t).\end{cases} \tag{2.3}$$

In order to make clear the net effect of the curve deformation over the whole time-interval $(0,\infty)$ it is interesting to see the limiting form of equation (2.3) as $t\to\infty$; we have

$$l(t)\sim\frac{tn}{2\pi}\int_0^{2\pi}\left[1+\left(\frac{\cos(\xi)}{n}\right)^2\right]^{1/2}\mathrm{d}\xi,\quad\text{as } t\to\infty, \tag{2.4}$$

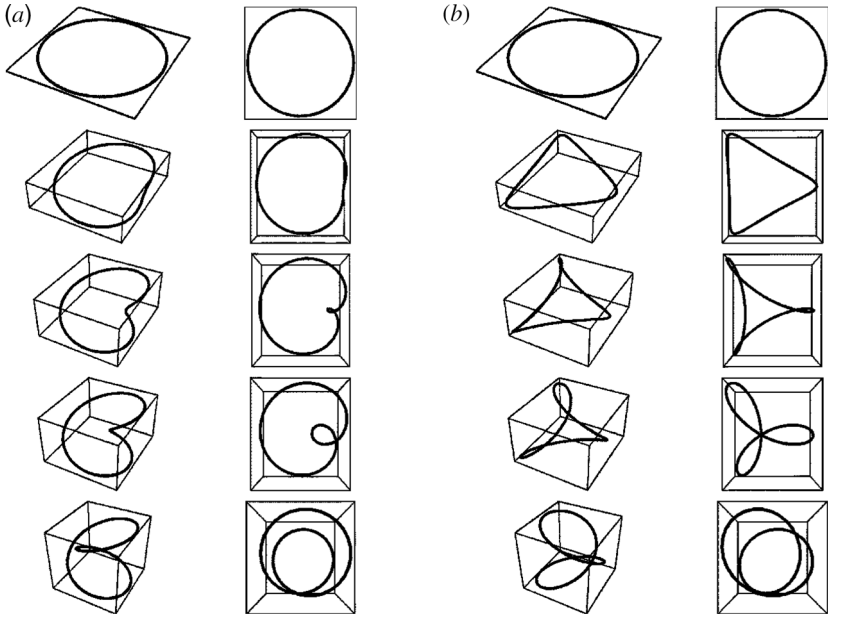

Figure 1. Side and top view of single coil formation generated by equations (2.3) from: (*a*) an epicycloid type of curve (with $a=c=+1$, $b=d=-1$) and (*b*) a hypocycloid type of curve (with $a=b=c=+1$, $d=-1$). Here, $m=1$ and $n=2$. In both cases, the single coil (bottom row, $t=6$) is produced from an initial circular configuration (top row, $t=0$); note that in (*a*) the coil evolves from one single loop, whereas in (*b*) it is generated from the simultaneous growth of three loop regions (second and third row). In both cases the writhing number Wr grows with time from 0 to the asymptotic value $Wr_{\max}=1$.

that clearly involves an elliptic integral of the second kind; hence, in the limit $t\to\infty$ we have:

$$\lim_{t\to\infty}\boldsymbol{X}(\xi,t):\quad\begin{cases}x\sim\dfrac{2\pi b\cos(n\xi)}{\int_0^{2\pi}[1+(\cos(\xi)/n)^2]^{1/2}\mathrm{d}\xi},\\[2ex] y\sim\dfrac{2\pi d\sin(n\xi)}{\int_0^{2\pi}[1+(\cos(\xi)/n)^2]^{1/2}\mathrm{d}\xi},\\[2ex] z\sim\dfrac{2\pi\sin(\xi)}{\int_0^{2\pi}[1+(\cos(\xi)/n)^2]^{1/2}\mathrm{d}\xi}.\end{cases}\tag{2.5}$$

(*a*) *Single coil formation*

For $m=1$ and $n=2$, equations (2.3) describe the evolution of $\mathcal{C}$ from a circular configuration to a three-dimensional curve with one single coil (see figure 1). According to the values of the parameters we have two different kinematics, shown in figure 1*a*,*b*, depending on whether the generatrix curve is an epicycloid or a hypocycloid. These two cases represent prototypes of coil formation. During evolution topology is conserved, so that Lk remains constant. For simplicity in the following (and in the rest of the paper) we shall take $Lk=1$. Since the original configuration is circular, equations (1.1) and (1.3) give $Wr=0$ and $Tw=1$ at $t=0$.

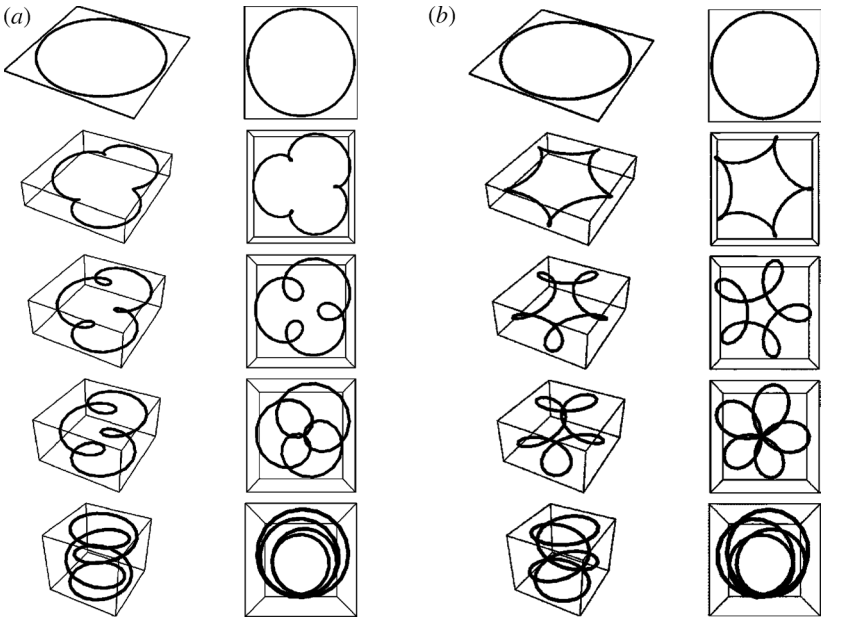

Figure 2. Side and top view of three coil formation generated by equations (2.3) from: (*a*) an epicycloid type of curve (with $a=c=+1$, $b=d=-1$) and (*b*) a hypocycloid type of curve (with $a=b=c=+1$, $d=-1$). Here, $m=1$ and $n=4$. In both cases three coils (bottom row, $t=6$) are produced from an initial circular configuration (top row, $t=0$); in (*a*) three coils evolve from three loop deformations, while in (*b*) the coils are generated from simultaneous growth of five loop regions (second and third row). Note that, in both cases we still have $Wr_{\max}=1$.

As t increases, the filament will form one single coil through the conversion of twist to writhe, according to the conservation of (1.1), and asymptotically (as $t\to\infty$) Tw will be completely converted to Wr (hence, in the limit, $Tw=0$, $Wr=1$).

From a topological viewpoint the evolutions of figure 1*a*,*b* are equivalent; there are, however, marked differences in the geometric way the coils form. In figure 1*a*, the filament writhes and coils simultaneously through one deformation shown by the diagrams in the second and third row. The coil springs from a localized loop region and grows out in the interior region. The second evolution, shown in figure 1*b*, is given by a hypocycloid generatrix: in this case there are three distinct locations where loop deformation occurs, from each of which a single coil develops; the three coils thus produced are equal, but opposite in sign (given by the relative position of their strands), so that eventually two of them cancel out and coalesce in a single arc; hence, from the three emerging loops, only one survives to form the final coil.

(*b*) *Multiple coils from plane circle*

For $m=1$ and $n=2k$ ($k\in\mathbb{N}\backslash 0$) we have $2k-1$ coils. Table 1 shows the types of generatrix curve according to the value of the parameters and Wr-range during evolution. For n odd, we have the simultaneous production and collision of an even number of coils, generated symmetrically along the curve; so we shall exclude these values of n. Figure 2 shows the two prototype evolutions given by equations (2.3) in the case of three coils. Note that in figure 2*b* (second and third row)

Table 2. Case $m=n-1$: types of generatrix curve for different values of parameters; now we have $|Wr|_{\max}=m$. (For the pseudo-epicycloid the range of the writhing number shown is attained for any $n\in\mathbb{N}$, whereas for the pseudo-hypocycloids $n\in\mathbb{N}$ can only be even; for $n\in\mathbb{N}$ odd, the relative Wr-range of the pseudo-hypocycloids is exchanged.)

generatrix curve	a	b	c	d	Wr-range
pseudo-epicycloid	$+1$	±1	±1	$+1$	$[-m,0]$
pseudo-hypocycloid	$+1$	∓1	±1	$+1$	$[-m,0]$
pseudo-epicycloid	$+1$	∓1	±1	-1	$[0,m]$
puesdo-hypocycloid	$+1$	±1	±1	-1	$[0,m]$

five loop regions contribute to the generation of only three coils: as in the case above, from five emerging loops, only three survive to the final coils. Moreover, due to the opposite sign of the surviving coils, the writhing number remains bounded between 0 and 1, with $Wr\to1$ as $t\to\infty$. In general, to produce $n-1$ coils the epicycloids generate $n-1$ loops and the hypocycloids $n+1$ loops. Note that $|Wr|_{\max}=1$ persists regardless the number of coils produced, for any $n=2k$.

(*c*) *Multiple coils from multiple coverings of plane circle*

For m, n ($m=n-1$), equations (2.3) give more elaborate curves generated by pseudo-epicycloid and pseudo-hypocycloid, where the generatrices coincide only partly with the classical plane curves. Here, the first $m-1$ coils are indeed instantly produced from m coverings of a plane circle, while the remaining coil is generated during the full evolution of the curve. In the transient, the pseudo-epicycloids generate one loop and the pseudo-hypocycloids $2n-1$ loops, while the writhing number grows from 0 to the asymptotic value of m (see table 2). Figure 3 shows the two prototype evolutions for two coil formation.

3. Comparative analysis of writhing rates

We compare the kinematics considered so far in terms of relative writhing rates. Typical behaviours are shown in figure 4. Top row diagrams refer to (*a*) epicycloid and (*b*) hypocycloid evolution shown in figure 1: for these cases we have $\lim_{t\to\infty}Wr=1$. Note that the bound $Wr_{\max}=1$ persists for any number of coils generated, as shown in table 1. Because of the conservation of $Lk=1$ (cf. equation (1.1)), this implies also a bound on the total twist Tw. The comparison between top diagrams shows that the change in writhing of the hypocycloid evolution is faster than that of the epicycloid, where higher values are attained at later times. Hence, the hypocycloid evolution is also quicker to relax total twist.

Similarly for the bottom diagrams of figure 4: the case (*a*) refers to the pseudo-epicycloid and the case (*b*) to the pseudo-hypocycloid evolution of figure 3. Here, the first $m-1$ coils are instantly produced from the m coverings of the plane circle and so Wr jumps instantaneously from 0 to $m-1$ as the curve evolves. In the case shown, we have $m=2$, so that Wr jumps suddenly to 1, tending then asymptotically to the limit value $Wr_{\max}=2$. In general, when $m=n-1$ the writhing

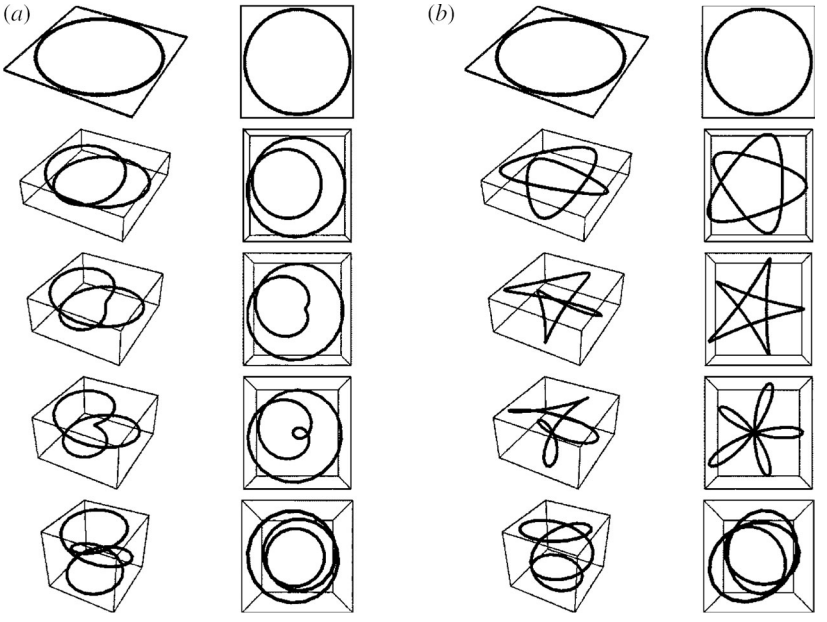

Figure 3. Side and top view of two coil formation given by equations (2.3) from: (*a*) pseudo-epicycloid generatrix (with $a=c=+1$, $b=d=-1$) and (*b*) pseudo-hypocycloid generatrix (with $a=\mathrm{b}=c=+1$, $d=-1$). Here $m=2$ and $n=3$. In (*a*) the first coil is produced instantly from a double covering of the plane circle, while the second coil is generated at later time (third row). In (*b*) five transient loop regions relax to two coils. In both cases the writhing number grows to attain the asymptotic value $Wr_{\max}=2$.

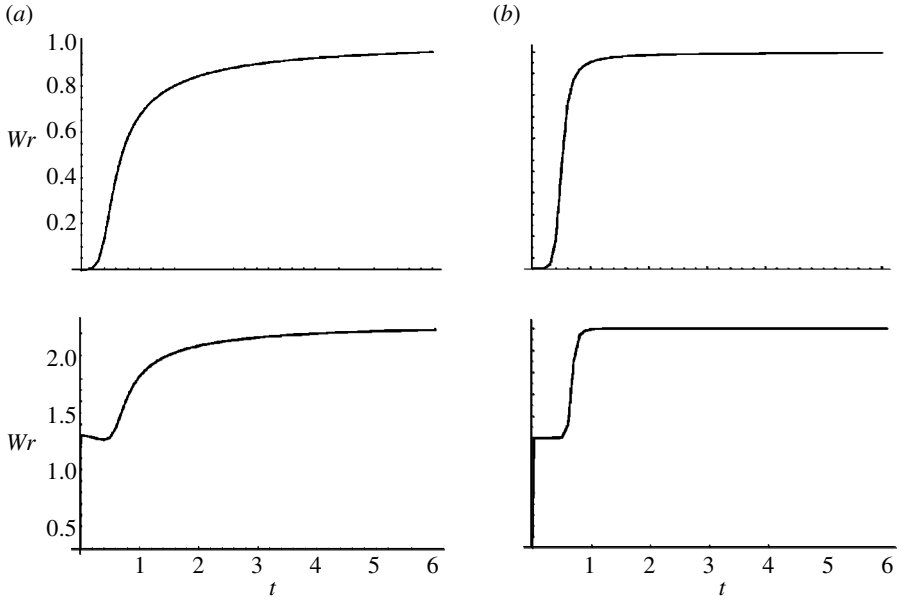

Figure 4. Writhing number Wr plotted against time. Top row diagrams refer to (*a*) epicycloid and (*b*) hypocycloid evolution of figure 1. Bottom row diagrams refer to (*a*) pseudo-epicycloid and (*b*) pseudo-hypocycloid evolution of figure 3.

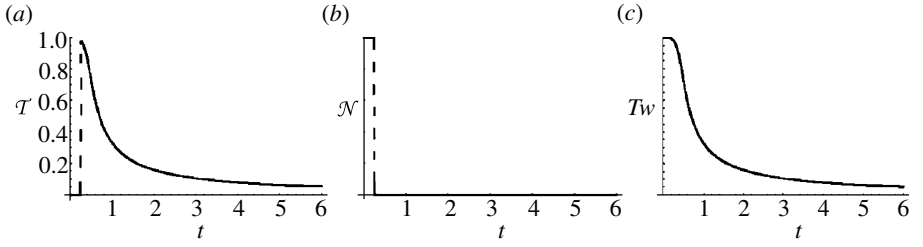

Figure 5. Diagrams of normalized (*a*) total torsion $\mathcal{T}$, (*b*) intrinsic twist $\mathcal{N}$, and (*c*) total twist Tw, plotted against time. The plots refer to the curve of figure 1*a*, but similar results hold true for any curve of the family of equations (2.3). Note that at the passage through the inflexion point (here at $\xi=0$, $t=0.25$), the discontinuities in $\mathcal{T}$ and $\mathcal{N}$ cancel out, so that the sum $\mathcal{T}+\mathcal{N}=Tw$ gives (*c*) a smooth function of ξ and t.

number has an upper bound given by $Wr_{\max}=m$. As in the previous case the growth of Wr to its limit value is much faster for the pseudo-hypocycloid than for the pseudo-epicycloid.

4. Loop deformation and inflexional states

All cases considered show that coiling originates from local writhing of the filament axis to form a loop region. This mechanism is generically performed by a loop deformation, known as Reidemeister type I move, that is associated with the exchange of twist and writhe. This mechanism was originally recognized by Călugăreanu (1961) and has also been analysed in detail by Moffatt & Ricca (1992), who showed that this local deformation consists invariably of a passage through an inflexional state, defined by vanishing curvature and local change of concavity of the curve. We must stress that the appearance of an inflexional state is a *generic* geometric feature, independent of the kinematics considered, and therefore it occurs during any coil formation. Moffatt & Ricca (1992) showed that at the point of inflexion the torsion is singular, but the singularity is integrable. The contribution from the integral of the total torsion through the inflexional state involves a jump $[\mathcal{T}]=1$ in total torsion, that must be compensated by an equal and opposite jump in the intrinsic twist, so that the twist number Tw (cf. equation (1.5)) remains a smooth function of ξ and t.

This situation is typified by the diagrams of figure 5, that refer to the evolution of the epicycloid generatrix of figure 1*a*. Similar results hold true for any curve of the family of equations (2.3). Since the initial conditions are given by $\mathcal{T}=0$ and $\mathcal{N}=1$, the initial total twist Tw is only given by pure intrinsic twist. As we see from figure 5*a*,*b*, passage through inflexion (that in this case occurs at $\xi=0$, $t=0.25$) leads to the complete conversion of one full intrinsic twist to total torsion. With reference to equations (2.3), if $\mathcal{N}(0)$ is the number of full turns of twist present initially, and N is the final number of coils produced, then $\mathcal{N}(0)-N=\mathcal{N}(\infty)$ is the number of intrinsic twists present in $\mathcal{F}$ in the limit $t\to\infty$, since in this limit total torsion is zero again. Inflexional deformations provide a mechanism for instantaneous, localized conversion of intrinsic twist to total

torsion, an action that, as we shall see in the §5, has important consequences on the energetics of the whole system.

An analysis of the occurrence of inflexional states is easily implemented for any specified kinematics (or dynamics). Given the equation $\boldsymbol{X}=\boldsymbol{X}=(\xi,\,t)$, curvature c and torsion τ are defined by

$$c(\xi,t)=\frac{\|\boldsymbol{X}'\times\boldsymbol{X}''\|}{\|\boldsymbol{X}'\|^3},\qquad \tau(\xi,t)=\frac{\boldsymbol{X}'\times\boldsymbol{X}''\cdot\boldsymbol{X}'''}{\|\boldsymbol{X}'\times\boldsymbol{X}''\|^2}. \tag{4.1}$$

Since, by definition, $c(\xi,\,t)\geq 0$ and a smooth function of ξ, quite simply inflexion points are found by requiring

$$c(\xi,t)=0,\qquad [c(\xi,t)]'=0,\qquad ([c(\xi,t)]''>0), \tag{4.2}$$

the second condition ensuring change of concavity at the inflexion. Solutions to equations (4.2) in the unknowns ξ and t determine location and occurrence of the inflexion points. For the sake of example, it is worth applying this criterion to detect inflexion in one of the cases considered. Let us take the curve of figure 1*a*; we have

$$c=\frac{2\sqrt{2}[1+35t^2+74t^4-6t(2+17t^2)\cos\xi+6t^2(3+t^2)\cos(2\xi)-2t^3\cos(3\xi)]^{1/2}}{[2+9t^2-8t\cos\xi+t^2\cos(2\xi)]^{3/2}}, \tag{4.3}$$

and

$$\tau=\frac{6t^2[4t\cos\xi-\cos(2\xi)]}{1+35t^2+74t^4-6t(2+17t^2)\cos\xi+6t^2(3+t^2)\cos(2\xi)-2t^3\cos(3\xi)}. \tag{4.4}$$

Thus, we find one inflexion point at $\xi=\xi_{\mathrm{i}}=0$ and $t=t_{\mathrm{i}}=0.25$; at these values the torsion (4.4) is singular (interestingly, we have $\tau(0,0.25)=4$, but $\lim_{t\to 0.25^{\pm}}\tau(0,t)=\infty$). We can check that the singularity is integrable by making a Taylor expansion about these values. Let us make the substitution $t=u+1/4$, so that $u\to 0$ as $t\to 0.25$; for ξ and u small, with $u\ll\xi$, asymptotically near the inflexion point we have

$$\tau(\xi,u)\sim\frac{72\xi^2+(192+480\xi^2)u+(1536+384\xi^2)u^2}{18\xi^2-192\xi^2u+(640+576\xi^2)u^2}. \tag{4.5}$$

Direct integration of equation (4.5) over a small interval $[\xi,\xi_0]$ centred at ξ_{i} shows that indeed this singularity is integrable:

$$\frac{1}{2\pi}\int_{-\xi_0}^{\xi_0}\tau(\xi,u)\|X'(\xi,u)\|\,\mathrm{d}\xi=\left\{\frac{3\xi_0^3(525+6560u+26656u^2)}{3-32u+96u^2}+\frac{6\xi_0(3375-15300u-128400u^2)}{(3-32u+96u^2)^2}\right.$$
$$\left.-\frac{2\sqrt{15}(-2025+58860u-211968u^2)\arctan\left[\xi_0[3(3-32u+96u^2)]^{1/2}/8\sqrt{5}u\right]}{(3-32u+96u^2)^{5/2}}\right\}(450\sqrt{5}\pi)^{-1}; \tag{4.6}$$

in the limit $u\to 0$, we have

$$[\mathcal{T}]=\left[\lim_{\xi_0\to 0}\frac{525\xi_0^3+2250\xi_0+450\sqrt{5}(\pm\pi/2)}{450\sqrt{5}\pi}\right]=1, \tag{4.7}$$

where $[\mathcal{T}]$ denotes the jump in $\mathcal{T}$ due to the passage through the inflexion point.

Table 3. Number of inflexion points (q_i), location (ξ_i) and occurrence (t_i) according to type of generatrix curve, m and n.

generatrix curve	m	n	q_i	ξ_i	t_i
epicycloid	1	even	$n-1$	$\{((p\pi)/(n-1))/p$ even, $p<2(n-1)\}$	$1/n^2$
hypocycloid	1	even	$n+1$	$\{((p\pi)/(n+1))/p$ odd, $p<2(n+1)\}$	$1/n^2$
pseudo-epicycloid	$n-1$	n	1	0	m^2/n^2
pseudo-hypocycloid	$n-1$	n	$m+n$	$\{((p\pi)/(m+n))/p$ even, $p<2(m+n)\}$	m^2/n^2

Similar considerations apply to the other kinematics. For instance, direct inspection of equations (2.3) gives the number of inflexion points, their location and occurrence for each type of generatrix curve; these are listed in table 3.

5. Energy contributions from curvature, torsion and mean twist

As we saw in the §4, filament coiling is generated by loop deformations that are invariably associated with passage through inflexion and a re-arrangement of the filament fibres through conversion of one turn of intrinsic twist to total torsion. In physical systems, information on the actual twist rate is often inaccessible or difficult to predict; however, estimates of the individual contributions from torsion and intrinsic twist to the energetics of the filament are not only desirable, but of practical importance, so that it is useful to analyse these contributions separately in terms of relative deformation energy.

For this purpose we adopt the simplest possible approach given by the linear elastic theory for a uniformly homogeneous and isotropic filament, of circular cross-section and inextensible length, with elastic characteristics given by bending rigidity K_b and torsional rigidity K_t. In general $\chi\in[1,1.5]$, with $\chi=K_\mathrm{b}/K_\mathrm{t}$. In our case the stress-strain relation leads to the conventional quadratic form of the deformation energy, given by

$$E = E_\mathrm{b} + E_\mathrm{t} = \frac{1}{2}\oint_{\mathcal{C}} [K_\mathrm{b}(c(\xi))^2 + K_\mathrm{t}(\Omega(\xi))^2]\,\|\boldsymbol{X}'(\xi)\|\,\mathrm{d}\xi, \tag{5.1}$$

where we assumed zero natural twist rate of the filament fibres. The deformation energy E is thus given by the sum of the bending energy E_b, due to curvature effects, and the torsional energy E_t, due to torsion and intrinsic twist. Indeed, by using (1.4) and (1.5), we get

$$E_\mathrm{t} = \frac{K_\mathrm{t}}{2}\oint_{\mathcal{C}} (\Omega(\xi))^2\,\|\boldsymbol{X}'(\xi)\|\,\mathrm{d}\xi = \frac{K_\mathrm{t}}{2}\oint_{\mathcal{C}} [\tau(\xi) + (\boldsymbol{\Theta}'(\xi))]^2\,\|\boldsymbol{X}'(\xi)\|\,\mathrm{d}\xi. \tag{5.2}$$

Contribution from pure torsion alone is evidently given by the *torsion* energy

$$E_\tau \equiv \frac{K_\mathrm{t}}{2}\oint_{C} [\tau(\xi)]^2\,\|\boldsymbol{X}'(\xi)\|\,\mathrm{d}\xi, \tag{5.3}$$

with E_b and E_τ providing information on the share of deformation energy associated with the geometry of the filament axis. For a comparative analysis it is convenient to normalize everything with respect to a reference energy E_0, that

we choose to be that given by the initial circular configuration of radius $R_0 = c_0^{-1} = 1$ and zero twist, that is

$$E_0 = \frac{K_\mathrm{b}}{2}\oint_{\mathcal{C}} c_0^2 \mathrm{d}s = \pi K_\mathrm{b}, \tag{5.4}$$

where s denotes here the usual arc-length. Thus the relative bending and torsion energy are given by

$$\left.\begin{aligned} \tilde{E}_\mathrm{b}(t) &= \frac{E_\mathrm{b}(t)}{E_0} = \frac{1}{2\pi}\oint_{\mathcal{C}} (c(\xi,t))^2 \|\boldsymbol{X}'(\xi)\| \mathrm{d}\xi, \\ \tilde{E}_\tau(t) &= \frac{E_\tau(t)}{E_0} = \frac{1}{2\pi}\oint_{\mathcal{C}} (\tau(\xi,t))^2 \|\boldsymbol{X}'(\xi)\| \mathrm{d}\xi, \end{aligned}\right\} \tag{5.5}$$

where, without loss of generality, we set $\chi = (K_\mathrm{b}/K_\mathrm{t}) = 1$.

On the other hand, a lower bound to the torsional energy E_t is found by applying the Cauchy–Schwarz integral inequality

$$\left(\oint_{\mathcal{C}} \Omega \mathrm{d}s\right)^2 \leq \left(\oint_{\mathcal{C}} \Omega^2 \mathrm{d}s\right)\left(\oint_{\mathcal{C}} \mathrm{d}s\right). \tag{5.6}$$

Hence,

$$\left(\oint_{\mathcal{C}} \Omega(\xi)\|\boldsymbol{X}'(\xi)\| \mathrm{d}\xi\right)^2 \leq 2\pi \oint_{\mathcal{C}} (\Omega(\xi))^2 \|\boldsymbol{X}'(\xi)\| \mathrm{d}\xi, \tag{5.7}$$

and by multiplying both sides by $(2\pi)^{-2}$ and using equations (5.2) and (1.4), we have

$$Tw^2 = (1 - Wr)^2 \leq \tilde{E}_\mathrm{t}, \tag{5.8}$$

where, from conservation of topology and linking number (cf. equation (1.1)), we used the usual condition $Lk = 1$; $\tilde{E}_\mathrm{t}$ denotes torsional energy normalized by E_0. The inequality (5.8) provides a lower bound on torsional energy from writhing information, and it has general validity. Moreover, if we assume *uniform* twist rate, i.e. $\Omega = \Omega_0$ constant, a reasonable assumption when we are in a state of minimum energy (away from inflexional deformations and energy localizations), then by equation (1.4) and the first of equation (5.2) the torsional energy takes the form of *mean twist* energy E_tw

$$Tw = \frac{1}{2\pi}\Omega_0 L = \Omega_0, \quad \rightarrow \quad E_\mathrm{tw} \equiv E_\mathrm{t}|_{\Omega_0} = \frac{K_\mathrm{t} L}{2}(\Omega_0)^2 = \pi K_\mathrm{t}(1 - Wr)^2, \tag{5.9}$$

that provides a useful relation for relaxed configurations. Thus

$$\tilde{E}_\mathrm{tw}(t) = \frac{\pi K_\mathrm{t}}{E_0}(1 - Wr(t))^2 = (1 - Wr(t))^2. \tag{5.10}$$

We can now make comparison between the epicycloid and the hypocycloid evolution of figure 1*a*,*b*. Diagrams of the relative energies are shown in figure 6*a* for the epicycloid type and in figure 6*b* for the hypocycloid type. By comparing the relative bending energies (top row), we can see that in both cases $\tilde{E}_\mathrm{b}$ grows from $\tilde{E}_\mathrm{b}(0) = 1$ to a maximum, flattening to a plateau region for large t. The limit value $\lim_{t\to\infty} \tilde{E}_\mathrm{b}(t) = 4$ is attained only when we take $f_3(t)$ to be a function rapidly decreasing to zero (see equations (2.3)): in this case, since the length $L = 2\pi$, the

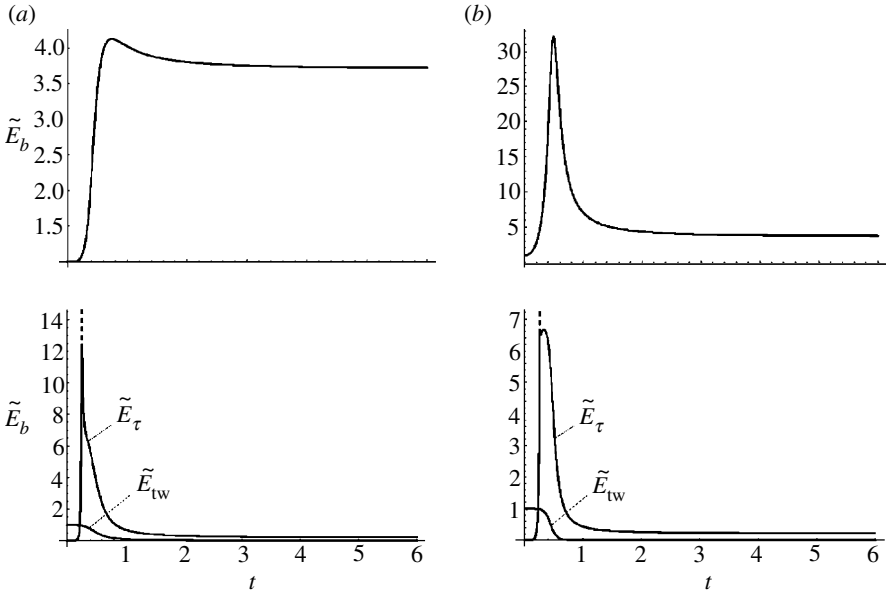

Figure 6. Diagrams of relative bending energy $\tilde{E}_{\rm b}$ (top row), mean twist energy $\tilde{E}_{\rm tw}$ and torsion energy $\tilde{E}_\tau$ (bottom row) for (*a*) epicycloid and (*b*) hypocycloid evolution of figure 1*a*,*b*. The singularity in $\tilde{E}_\tau$ is indicated by a dashed line.

curve will asymptotically tend to a double covering of the circle of radius 1/2. Note also the marked difference between the values of $\tilde{E}_{\rm b}$ for the two curves, due to the different mechanism of coil formation; in the hypocycloid case (see figure 6*b*) it is indeed the generation of three coils in the transient stage (see the discussion in §2) that is responsible for the high values of $\tilde{E}_{\rm b}$.

The diagrams of $\tilde{E}_{\rm tw}$ (bottom row) do not show any significant difference (having taken account of the different scales) between the two kinematics; the change in mean twist energy is obviously related to the change in the filament writhing, and evidently $\tilde{E}_{\rm tw}\to 0$ as $Wr\to 1$.

Finally, let us consider the torsion energy. As expected, both diagrams show a singularity at the inflexion point, at $t=0.25$. As we saw in §4 torsion is indeed singular at the inflexion point, but the singularity is integrable; in the case of $\tilde{E}_\tau$, however, the integrand is a quadratic function of torsion (it is actually just the squared value), which makes $\tilde{E}_\tau$ non-integrable. This can be easily verified by direct inspection of equation (5.3) as $t\to 0.25$. A simpler example of this singular behaviour is provided by the (generic) inflexional model proposed by Moffatt & Ricca (1992): from there, we have

$$\boldsymbol{X}(s,t)=\left(s-\frac{2}{3}t^2s^3,ts^2,s^3\right),\quad\text{and}\quad\tau(s,t)\sim\frac{3t}{t^2+9s^2},\tag{5.11}$$

with inflexion centred at $s=0$ and $t=0$. The contribution to torsion energy from any small interval $[-s_0,s_0]$ is thus given by

$$\frac{1}{\pi}\int_0^{s_0}\left(\frac{3t}{t^2+9s^2}\right)^2{\rm d}s=\frac{3}{\pi}\left[\frac{3s_0t}{9s_0^2+t^2}+\arctan\left(\frac{3s_0}{t}\right)\right](2t)^{-1}.\tag{5.12}$$

Hence, irrespective of the value of s_0, as t goes through zero we have

$$\lim_{t\to 0^{\pm}} E_\tau(0,t) = \lim_{t\to 0^{\pm}} \frac{\pm 3/4}{t} = +\infty. \tag{5.13}$$

The singularity in torsion energy is therefore related to the singular behaviour of torsion and, as discussed in §4, it is essentially due to the 'artificial' decomposition of Tw, a smooth function in ξ and t, into $\mathcal{T}$ and $\mathcal{N}$. In physical terms, however, *there is no singularity*, since there is an equal and opposite contribution from the intrinsic twist (not shown in diagrams) to compensate and eliminate the singularity (cf. diagram of figure 5*c*). Both diagrams show an increase of E_τ from zero (since at $t=0$ torsion is identically zero) to the inflexional deformation, followed, afterwards, by a gradual decrease to a plateau region. The limit value $\lim_{t\to\infty}\tilde{E}_\tau(t)=0$ is attained only when we take $f_3(t)$ to be a function rapidly decreasing to zero (see again equations (2.3)). Note also that, contrary to bending energy, both kinematics show similar localization of torsion energy, in terms of absolute values and spread. Anyway, a comparison between these diagrams shows that both epicycloid and pseudo-epicycloid evolutions are energetically much more effective than their sister kinematics, with much lower deformation energy rates.

It is also interesting to find out how much twist is needed in a circular filament to make it jump to the coiled state. Of course the transition occurs only if a 'deformation path' exists on which the total energy is monotonic decreasing. This can be easily checked by analysing the behaviour of $\tilde{E}_{\rm b}(t)+\tilde{E}_{\rm tw}(t)$ and comparing the values at the initial and final stage of evolution. In the simplest case of the epicycloid evolution of figure 1*a* we find that for $Tw\geq 6$ the total energy is always decreasing, hence favouring the transition to the coiled state. This behaviour seems to persist for the other cases, where, as coiling complexity increases, the minimum twist value necessary for the transition increases considerably in relation to the extremely high values of the bending energy. Finer analyses that would take into account contact or repulsive forces (to avoid self-crossings of the filament strands) would certainly be worth exploring.

6. Compactibility and packing rate

In many physical situations filamentary structures need to be highly packed in small volumes. On microscopic scales, for example, the human DNA is compacted in chromosomes by a factor of about 10 000, and it may be confined into a scroll of protein with packing ratio given by $D/L=O(10^{-5})$, where D and L denote typical sizes of the proteic region and DNA length (Coulombe & Burton 1999). On the other hand, on macroscopic scales, for instance in astrophysical flows, the compaction of magnetic fields in small regions leads naturally to an intensification of the average field, a process that can be associated with dynamo action (for example, through a stretch-twist-fold process, as proposed by Moffatt & Proctor 1985; see also Childress & Gilbert 1995).

We like to compare the kinematics considered here to quantify compactibility and packing rate in the light of possible applications. In the case of the generation of a single coil, at $t=0$ we have $L=2\pi R_0=2\pi$; when the coil is fully formed, the filament centreline will tend, on average, to a double covering of

a circle ofradius R. Since L is kept constant, the average radius of the new curve will, in the limit $t\rightarrow\infty$, be half of the original, that in our case corresponds to $R=1/2$. In general, if N is the total number of coils produced, then we have:

$$L = 2\pi = (N+1)2\pi R \rightarrow R = \frac{1}{N+1}. \tag{6.1}$$

In general, then, if $N=N(t)$ is the number of coils produced per unit time, the *packing rate* $\rho=\rho(t)$ will be given by $O(t)=[N(t)+1]^{-1}$.

In conclusion, by analysing competing kinematic models of writhing and coiling formation, based on epicycloid and hypocycloid evolutions, we showed how efficiency of coil formation and compaction mechanisms depend on writhing rates, relative bending, torsion and mean twist energy. In particular, we demonstrated that when coiling is produced by an epicycloid generatrix writhing rates are lower than those for a hypocycloid evolution, at the expense of a much higher deformation energy. Moreover, some of the kinematics considered have $\mathrm{Wr}_{\max}=1$, regardless the number of coils formed. Since the linking number Lk is invariant, the above bound on the writhing number implies a bound on the total twist Tw: this means that even when multiple coils are formed, the total twist remains bounded, irrespective of the number of coils produced. This is naturally reflected on the bound on the twist energy, which physically is evidently an important aspect.

The occurrence and multiple appearance of inflexional configurations has been analysed in detail. We showed that passage through inflexion must involve a very high, localized distortion of the filament fibres, through localization of their intrinsic twist. This mechanism has physical relevance, especially in the context of elastic rod theory, where the deformation process is mechanically justified by a writhing instability (Zajac 1962) and is responsible for the relaxation of highly twisted configurations tosupercoiled states (Ricca 1995; Klapper 1996). In the case of macromolecules, where conformational information (due to geometry) and transcriptional mechanisms (associated with the interaction of the filament strands) are inherently associated with geometric and structural properties of the filament model, high values of torsion and intrinsic twist, concentrated in short segments, as well as packing, play surely an important role in many functional and biological aspects. Thus, the results presented here, and the considerations above, are likely to be relevant in those processes where there is a strong relation between structural complexity and localization of energy (Ricca 2005). Work is in progress to apply these results to investigate further localized coiling and its effects on DNA compaction (Ricca & Maggioni submitted) and magnetic dynamo actions.

We would like to thank Keith Moffatt for his comments on a preliminary draft of this paper. R.L. Ricca acknowledges financial support from Italy's MIUR (D.M. 26.01.01, n. 13 'Incentivazione alla mobilità di studiosi stranieri e italiani residenti all'estero' and COFIN2004-PRIN Project 'Mathematical Models for DNA Dynamics $M^2\times D^{2}$') and The Royal Society of London (Joint Project Grant under the European Science Exchange Programme).

References

Arganbright, D. E. 1993 *Practical handbook of spreadsheet curves and geometric constructions.* Boca Raton, FL: CRC Press.

Baker, D. 2000 A surprising simplicity to protein folding. *Nature* **405**, 39–42. (doi:10.1038/35011000)

Călugăreanu, G. 1961 Sur les classes d'isotopie des nœuds tridimensionnels et leurs invariants. *Czechoslovak Math. J.* **11**, 588–625.

Calladine, C. R. & Drew, H. R. 1992 *Understanding DNA*. New York, NY: Academic Press.

Childress, S. & Gilbert, A. D. 1995 *Stretch, twist, fold: the fast dynamo*. Berlin, Germany: Springer.

Coulombe, B. & Burton, Z. F. 1999 DNA bending and wrapping around RNA polymerase: a 'revolutionary' model describing transcriptional mechanisms. *Microbiol. Mol. Biol. Rev.* **63**, 457–478.

Fuller, F. B. 1971 The writhing number of a space curve. *Proc. Natl Acad. Sci. USA* **68**, 815–819.

Klapper, I. 1996 Biological applications of the dynamics of twisted elastic rods. *J. Comp. Phys.* **125**, 325–337. (doi:10.1006/jcph.1996.0097)

Lockwood, E. H. 1961 *A book of curves*. Cambridge, UK: Cambridge University Press.

Moffatt, H. K. & Proctor, M. R. E. 1985 Topological constraints associated with fast dynamo action. *J. Fluid Mech.* **154**, 493–507.

Moffatt, H. K. & Ricca, R. L. 1992 Helicity and the Călugăreanu invariant. *Proc. R. Soc. A* **439**, 411–429.

Ricca, R. L. 1995 The energy spectrum of a twisted flexible string under elastic relaxation. *J. Phys. A: Math. Gen.* **28**, 2335–2352. (doi:10.1088/0305-4470/28/8/024)

Ricca, R. L. 2005 Structural complexity. In *Encyclopedia of nonlinear science* (ed. A. Scott), pp. 885–887. New York, NY and London, UK: Routledge.

Ricca, R. L. & Maggioni, F. Submitted. Multiple folding and packing in DNA modeling. *Comput. Math. Appl.*

Stasiak, A. 1996 Circular DNA. In *Large ring molecules* (ed. J. A. Semlyen), pp. 43–97. Chichester, UK: Wiley.

White, J. H. 1969 Self-linking and the Gauss integral in higher dimensions. *Am. J. Math.* **91**, 693–728.

Zajac, E. E. 1962 Stability of two planar loop elasticas. *J. Appl. Mech.* **29**, 136–142.

Zhang, P., Tobias, I. & Olson, W. K. 1994 Computer simulation of protein-induced structural changes in closed circular DNA. *J. Mol. Biol.* **242**, 271–290. (doi:10.1006/jmbi.1994.1578)